Spectroscopic factors for nucleon knock-out from ^{16}O at small missing energy

W. J. W. Geurts and K. Allaart
Department of Physics and Astronomy, Vrije Universiteit, De Boelelaan 1081, 1081 HV Amsterdam, The Netherlands

W. H. Dickhoff
Department of Physics, Washington University, St. Louis, Missouri 63130

H. Müther
Institut für Theoretische Physik, Universität Tübingen, Auf der Morgenstelle 14, D-72076 Tübingen, Germany
(Received 22 November 1995)

Spectroscopic factors for one-nucleon knock-out from ^{16}O are calculated for states with low excitation energy in ^{15}N with the Bonn-*C* potential. A method is proposed to deal with both short- and long-range correlations consistently. For this purpose a Green's function formalism is used and the self-energy in the Dyson equation is approximated as the sum of an energy-dependent Hartree-Fock (HF) term and dispersion and correlation terms of higher order in the *G*-matrix interaction. This *G* matrix is obtained by solving the Bethe-Goldstone equation with a Pauli operator which excludes just the model space treated in the subsequent calculation of the self-energy. The energy dependence of the HF energies induces an additional reduction of the spectroscopic factors for quasiparticle states close to the Fermi level by about 10%. Experimental data may signal the need of some further improvement in the treatment of intermediate- and long-range correlations. [S0556-2813(96)04105-2]

PACS number(s): 21.10.Jx, 21.30.Fe, 21.60.Jz, 27.20.+n

I. INTRODUCTION

In several $(e,e'p)$ experiments [1–4], a substantial fragmentation of the one-nucleon knock-out strength has been observed. In various calculations of the one-nucleon spectral function at low energies [5–8] this fragmentation has been shown to be due to long-range correlations. It was also noticed, however, that an additional mechanism must be acting which reduces the spectral strength in the low-energy region, especially the (main) quasiparticle peak. The effect of short-range correlations represents a prime candidate for the explanation of this discrepancy between the calculations and the data. Calculations in nuclear matter [9] show that this effect is about 15%.

In other theoretical studies, the spectral function calculated for nuclear matter was transformed to the finite nucleus by a local density approximation [10]. In these calculations, spectroscopic factors for the states around the Fermi level came out even considerably lower than deduced from the data. This is possibly due to double counting when the effect of surface vibrations deduced from phenomenological optical potentials is added on top of that deduced from nuclear matter.

The quasihole wave function of ^{16}O was also calculated with variational methods [11]. These results were compatible with a 20% (10%) reduction of the spectroscopic factor depending on whether center-of-mass motion was taken care of or not. Also in Brueckner-Hartree-Fock calculations [12], neglecting center-of-mass motion, a value of 0.91 for the hole spectroscopic factor was found.

The reason why long- and short-range correlations were not dealt with simultaneously in a calculation for a finite nucleus so far is that an excessively large (shell) model space would be required to include the scattering by the strongly repulsive cores of a realistic *NN* interaction. For this reason one normally deals with a limited model space, of say four or five major shells, and a Brueckner *G* matrix as an effective interaction. By construction the *G* matrix, which is the solution of a Bethe-Goldstone equation, is energy dependent. This energy dependence is rather weak, however, as compared to that of the dispersion effects which at low energies contribute pole terms to the self-energy. Therefore, in low-energy nuclear structure calculations, the *G* matrix is usually considered as a static, i.e., energy-independent interaction. In the present work however, it is our aim to take its energy dependence into account and study its effect on the spectral function at low energies. It may be expected that by doing so, one accounts to a good approximation for the effects of the short-range correlations, which were treated in the construction of the *G* matrix. In this sense, our results do incorporate effects of both short- and long-range correlations consistently.

The computational procedure and input are described in Sec. II. Results for the one-body spectral function of ^{16}O are presented and compared with the available data in Sec. III. Section IV contains a short summary and conclusions.

II. GREEN'S FUNCTION METHOD: CALCULATION OF THE SELF-ENERGY

The spectroscopic factors for the one-nucleon removal are defined as the square of the overlap of the ground state wave function from which a particle in orbit α is removed, with the states of the final nucleus

$$S_n(\alpha)=|\langle\Psi_n^{A-1}|a_\alpha|\Psi_0^A\rangle|^2. \quad (1)$$

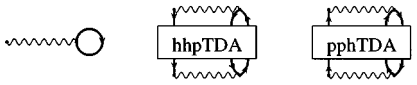

FIG. 1. Graphical representation of some contributions to the irreducible self-energy Σ^*, that appear in the Dyson equation (3). The thick lines indicate single-particle propagators g, that are solutions of the Dyson equation. The wiggly lines denote the G-matrix interaction. The first diagram is the Hartree-Fock contribution (5), the second and third diagrams include two-particle–one-hole and two-hole–one-particle interactions in Tamm-Dancoff approximations, cf. Eq. (10).

These may be obtained from the diagonal elements of the one-body Green's function [13,14]

$$g_{\alpha\beta}(\omega)=\sum_n \frac{\langle\Psi_0^A|a_\beta|\Psi_n^{A-1}\rangle\langle\Psi_n^{A-1}|a_\alpha^\dagger|\Psi_0^A\rangle}{\omega-(E_0^A-E_m^{A-1})-i\eta} + \sum_m \frac{\langle\Psi_0^A|a_\alpha^\dagger|\Psi_m^{A+1}\rangle\langle\Psi_m^{A+1}|a_\beta|\Psi_0^A\rangle}{\omega-(E_n^{A+1}-E_0^A)+i\eta}. \quad (2)$$

This also contains amplitudes for the addition of one particle. The interesting property of the Green's function is that it may be calculated by solving the Dyson equation

$$g_{\alpha\beta}(\omega)=g^0_{\alpha\beta}(\omega)+\sum_{\gamma\delta} g^0_{\alpha\gamma}(\omega)\Sigma^*_{\gamma\delta}(\omega)g_{\delta\beta}(\omega), \quad (3)$$

with the irreducible self-energy $\Sigma^*(\omega)$. The latter acts as an effective, energy-dependent, potential for which formally a Feynman-Dyson series expansion is given [13,14], but for which in practice some approximation must be adopted.

For shell model orbits $\alpha=(n_a,l_a,j_a,m_a)$ just below the Fermi energy, there is usually one final state Ψ_n^{A-1} for which the spectroscopic factor is large, i.e., comparable with unity. In calculations within a finite model space, one finds that these orbits are to a good approximation the (Brueckner) Hartree-Fock orbits. Other orbits, with different radial quantum numbers, contribute little at low energy. This agrees with the experimental finding [1–4] that the missing momentum distributions in $(e,e'p)$ reactions are the same for all final states with the same spin and parity and low excitation energy. So these may be interpreted as fractions of the knock-out strength from the same shell model orbit. Therefore the Green's function (2) may be treated as diagonal in the orbital indices within a suitably chosen shell model basis. The spectroscopic factors are then obtained from the normalization condition

$$|\langle\Psi_m^{A-1}|a_\alpha|\Psi_0^A\rangle|^2=\left(1-\frac{\partial\Sigma^*_\alpha(\omega)}{\partial\omega}\right)^{-1}_{\omega=E_0^A-E_m^{A-1}}. \quad (4)$$

The irreducible self-energy Σ^* is approximated here by the diagrams of Fig. 1, which are discussed below. In the Hartree-Fock (HF) diagram the energy dependence of the G matrix simulates the effect of short-range correlations at low energy; the 2p1h and 2h1p propagator diagrams should account for the fragmentation of strength at low energy due to long-range correlations. This 2p1h Tamm-Dancoff approximation (TDA) self-energy has been studied in [15].

A. Energy dependence of (Brueckner) HF self-energy

The contribution to the irreducible self-energy of first order in the G matrix, depicted in the Hartree-Fock diagram of Fig. 1, is given by

$$\Sigma^{\rm HF}_{\alpha\beta}(\omega)=i\sum_{\gamma\delta}\int\frac{d\omega'}{2\pi}G_{\alpha\gamma\beta\delta}(\omega+\omega')g_{\gamma\delta}(\omega'), \quad (5)$$

where the proper energy dependence of the G matrix is taken into account. This G-matrix interaction is constructed for the finite nucleus ^{16}O by the method described in [16]. With this method the Bethe-Goldstone equation for the G matrix

$$G=V+V\frac{\hat{Q}}{\omega-H_0+i\eta}G, \quad (6)$$

is solved for a set of starting energies ω ranging from -110 to -5 MeV. The Pauli operator $\hat{Q}$ excludes a shell model space of the $1s$ up to $2p1f$ harmonic oscillator states, with oscillator parameter $b=1.76$ fm. The (long-range) correlations within this excluded space are treated later, by the methods discussed in the next section.

The NN interaction V adopted in this work is the Bonn-C potential [17]. We expect that other realistic potentials will yield results which are similar to the ones obtained with this potential. Realistic potentials may differ considerably in the central repulsion at short distance as well as in the tensor part. In order to fit the same NN phase shifts and the binding energy of the deuteron, however, a stronger central repulsion requires a stronger tensor force, which in turn yields a lager d-state probability of the deuteron wave function. For the Bonn-C potential the d-state probability of the deuteron wave function is 5.6%, close to that for the Paris potential [18] and the Argonne potential [19] and intermediate between the 6.5% for the Reid soft core potential [20] and 4.4% for the very ''soft'' Bonn-A potential.

The depletion of orbits below the Fermi level by short-range and tensor correlations is not very sensitive to the adopted NN potential. Calculations for nuclear matter at a Fermi momentum $k_F=1.36$ fm^{-1} yield an average occupation probability for states below the Fermi level of 0.83 for the Reid potential and 0.86 for the OBEP-B interaction [21]. Occupation numbers for states with small momenta obtained with different potentials and using various methods are hardly distinguishable. Employing Brueckner theory [22] and the Paris potential an occupation number of 0.82 is obtained, while recent calculations with correlated basis functions and the Urbana v14 potential [23] yield 0.83 [24] and Green's function methods with the Reid potential 0.83 [25].

In the present approach the depletion of orbits by the short-range correlations is introduced through the energy dependence of the G matrix in the HF self-energy. In that case also the single-particle energies in the HF propagator,

$$g^{\rm HF}_\alpha(\omega)=\left[\frac{\theta(\alpha-F)}{\omega-\varepsilon^{\rm HF}_\alpha(\omega)+i\eta}+\frac{\theta(F-\alpha)}{\omega-\varepsilon^{\rm HF}_\alpha(\omega)-i\eta}\right], \quad (7)$$

become energy dependent:

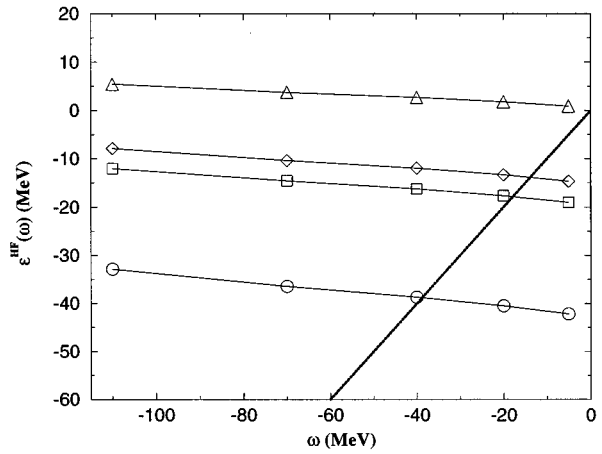

FIG. 2. Values of the HF energies (8) for $\omega=-110$, -70, -40, -20, and -5 MeV are plotted for various shells: $1s(1/2)$ (circles), $1p(3/2)$ (squares), $1p(1/2)$ (diamonds), and $1d(5/2)$ (triangles). Intersection of the interpolated curves with the dotted line yields the self-consistent solution $\omega=\varepsilon_\alpha^{\rm HF}(\omega)$ of the HF energies.

$$\varepsilon_\alpha^{\rm HF}(\omega)=T_\alpha+\Sigma_\alpha^{\rm HF}(\omega)$$
$$=\tfrac{1}{2}\hbar\Omega^2(2n_\alpha+l_\alpha+\tfrac{3}{2})+\sum_{\gamma<F}\mathrm{G}_{\alpha\gamma\alpha\gamma}(\omega+\varepsilon_\gamma^{\rm HF}). \tag{8}$$

The kinetic energy T_α is calculated for the basis of harmonic oscillator states ($\hbar\Omega=$ 14 MeV), using the same basis in which also the Bethe-Goldstone equation was solved. The sum in (8) runs over all states below the Fermi level and the self-consistency relation $\omega=\varepsilon_\alpha^{\rm HF}(\omega)$ should be imposed. The energy dependence in the range of energies around the Fermi level is very smooth, so the self-consistent solutions of (8) can be obtained by interpolation, as shown in Fig. 2. If the self-energy Σ^* is restricted to the HF term only, the slope of the curves at the crossing points in Fig. 2 now causes a reduction of pole strength (4) already in the HF approximation. In the present calculation this reduction is 5–7 %. It means that the short-range correlations treated in Brueckner-Hartree-Fock approximation give rise to a high-energy (and momentum) tail of the spectral function which is of about this magnitude, and is invisible in the low-energy spectra. This result is consistent with the numbers obtained in the direct calculation of [26], where the focus is on the high-momentum part of the spectral function.

B. Long-range correlations included by 2p1h TDA self-energy

The fragmentation of particle removal strength over several states in the low-energy domain is mainly caused by the mixing of the one-hole with two-hole–one-particle (2h1p) configurations. This may be described by including contributions depicted on the right in Fig. 1 to the self-energy Σ^*. In the simplest diagram of second order in the interaction, one has just three noninteracting lines as the intermediate stage. That approximation was employed in [5]. If no further interaction between the three lines is included, one neglects a possible formation of intermediate collective excitations, i.e., of typical particle-plus-phonon states. In [27] this formation of particle-hole or hole-hole collective states among the three lines was described in the random phase approximation (RPA), but unsatisfactory features of that method turned up. The Pauli principle between the collective pair and the third fermion is neglected, like in most phenomenological particle-phonon coupling models. Moreover, some of the RPA phonons, to which the hole was coupled, became unstable with the G-matrix interaction and were simply discarded in [27]. Therefore an alternative approach, in which these problems are avoided, is adopted here. This was first discussed in [28,29] and applied recently [15] in a study of the spectral function of ^{48}Ca. In this approach one sums the self-energy to all orders in the interaction, but with the restriction that at the intermediate stages there are always just three lines. For this reason it was coined the ''Faddeev'' approximation in [29]. Diagrams with more than two holes and one particle at a time are neglected. Those with only one line as an intermediate step *must* be rejected, because otherwise the self-energy is no longer irreducible [13,14]. As discussed in more detail in [15,28,29], this Faddeev approximation for the three propagating lines corresponds to a full diagonalization of the interaction within the 2p1h and 2h1p model spaces. This is what is usually called the 2p1h (2h1p) Tamm-Dancoff approximation. The diagonalization yields the eigenvalues ω^ν, numbered by the upper index ν. With the corresponding eigenvectors b^ν_{lmn}, in which the indices l, m, and n denote the particle and hole quantum numbers, the propagation of the three interacting lines in the self-energy diagrams, Fig. 1, is then represented by the irreducible propagator [15]

$$\overline{R}_{lmn;pqs}(\omega)=\sum_\nu \frac{b^\nu_{lmn}b^\nu_{pqs}}{\omega-\omega^\nu}. \tag{9}$$

The contribution of the complete diagrams to the irreducible self-energy Σ^* is obtained by sandwiching this expression with the G-matrix interactions at the beginning and at the end:

$$\Sigma^*_{\alpha\beta}(\omega)=\Sigma^{\rm HF}_{\alpha\beta}(\omega)+\sum_{lmn;pqs}\ \tfrac{1}{2}G_{\alpha lmn}\overline{R}_{mnl;pqs}(\omega)\ \tfrac{1}{2}G_{pq\beta s}\,. \tag{10}$$

In principle the calculation of the eigenvalues and eigenvectors of the Hamiltonian within the 2p1h and 2h1p spaces, leading to $\overline{R}$ (9), should be performed with the energy-dependent G-matrix elements and single-particle energies. This is a cumbersome procedure and in fact unnecessary for practical purposes. A simpler procedure is justified by the following two observations. First, the ω dependence of the G matrix and the HF energies is weak and smooth as compared to the pole structure of $\overline{R}$ (9). So a large amount of computational effort may be saved by calculating these poles and eigenvectors in (9) with a fixed ''starting energy'' for the G matrix, for which a value of -40 MeV was taken as a suitable average for a 2h1p state. For the 2p1h states one would prefer a higher starting energy, but these states are less important for the description of the experimentally measured hole spectral function. The second observation is that the calculation of the self-energy and the procedure of solving the Dyson equation become effectively decoupled when

TABLE I. Shell model space $\mathscr{M}$ for ^{16}O, in which the self-energies (10) are calculated. The listed single-particle energies are obtained by the procedure sketched in Fig. 2 and further discussed at the end of Sec. II B.

Shell	Proton energy (MeV)	Neutron energy (MeV)
$1s\frac{1}{2}$	−35.0	−40.0
$1p\frac{3}{2}$	−18.5	−21.8
$1p\frac{1}{2}$	−12.1	−15.7
$1d\frac{5}{2}$	−0.6	−4.1
$1d\frac{3}{2}$	4.4	0.9
$2s\frac{1}{2}$	−0.1	−3.3
$1f\frac{7}{2}$	17.4	14.0
$1f\frac{5}{2}$	23.5	20.2
$2p\frac{3}{2}$	16.0	12.4
$2p\frac{1}{2}$	17.7	14.3

the condition is imposed that, for the shells around the Fermi level, the calculated quasiparticle energies must correspond to the experimental ones. The method adopted here is to calculate the eigenvalues ω^ν and eigenvectors b^ν_{lmn} with the single-particle energies (8) and G($\omega=-40$ MeV). Next, the Dyson equation (3) is solved with the self-energies (10) within the model space of four harmonic oscillator major shells. If the energies of the main quasiparticle peaks around the Fermi level differ appreciably from the experimental values, the corresponding single-particle energy $\varepsilon^{\rm HF}_\alpha(\omega)$ is shifted by a constant, which has no influence on the derivative in Fig. 2, and the whole procedure is repeated. As a result the single-particle values of Table I were obtained. Not many iterations are needed because the adjustments are small. Moreover, high precision at this point is not meaningful in view of the various approximations and slight inconsistencies that are still inherent in the method and which are shortly addressed in the next section.

C. Self-consistency and sum rule check

Besides the use of a fixed ω value for the G-matrix interaction in the calculation of the 2p1h and 2h1p amplitudes, there is a more important problem if one wishes to solve the Dyson equation with a self-consistent self-energy. This arises as soon as the 2p1h propagator in Fig. 1 is no longer restricted to its Faddeev (TDA) form, but consists of diagrams that involve ''dressed'' nucleons, i.e., nucleons fully interacting with all other nucleons. These dressed nucleons are then described with a fragmented one-body propagator and no longer with the single-pole propagator of Eq. (7). Now the self-energy (10) depends on the solution of the Dyson equation in which it appears. The use of an iterative scheme, where the propagator of the $(n-1)$th step is used as input for the calculation of the self-energy in the nth step becomes very cumbersome, because in each step the number of poles increases and thereby the complexity of the the expressions for the self-energy. The self-consistency can only be studied for simple approximations of the self-energy, e.g., without further interaction between the three lines in Fig. 1. This has been applied by Van Neck [7], who represented the propagators in a limited set of energy bins. A different approach to reach a certain self-consistency is the basis generated by the Lanczos (BAGEL) [8] method. In this method, the Dyson equation is written as a matrix equation, within the space composed of the one-hole state and the 2h1p states. The most important eigenvectors are then filtered out by the Lanczos method. A self-consistent calculation of the one-body propagator for the tin isotopes with a pairing force and a 2p1h TDA self-energy is given in [30].

TABLE II. Influence of the energy dependence of the Hartree-Fock energies in the calculation of one-proton removal or addition strengths for ^{16}O. Listed are the proton removal strengths summed over all final states (hole), as a fraction of the values for the independent-particle shell model and the same for the proton-addition strength (particle). Also the strength for the single state with largest spectroscopic factor (main peak) is given.

	Energy dependent $\epsilon^{\rm HF}$			Energy independent $\epsilon^{\rm HF}$		
Shell	Hole	Particle	Main peak	Hole	Particle	Main peak
$1d\frac{3}{2}$	0.035	0.914	0.82	0.037	0.963	0.87
$1d\frac{5}{2}$	0.034	0.913	0.86	0.037	0.963	0.91
$1p\frac{1}{2}$	0.837	0.094	0.77	0.903	0.097	0.83
$1p\frac{3}{2}$	0.879	0.052	0.76	0.945	0.055	0.82
$1s\frac{1}{2}$	0.880	0.043	—	0.954	0.046	—

As a consequence of the lack of self-consistency, elementary sum rules may be violated. For a given orbit, the sum of all removal and addition spectroscopic factors, i.e., of all residues of the corresponding Green's functions, must be unity. In the present case, however, this sum is already smaller in HF approximation. As a consequence of the energy dependence of the G matrix, the strength at very high energies due to short-range correlations is hidden. So to assess the violation of the sum rule due to the lack of self-consistency, we have also performed a calculation without any energy dependence in the HF part. In that case the violation appeared to be only of the order of 10^{-8}.

III. HOLE SPECTRAL FUNCTIONS: RESULTS

With the self-energies (10), constructed with the G matrix of the Bonn-C potential within the model space of four major oscillator shells, the Dyson equation (3) may be solved and the spectroscopic factors (4) obtained. These are hereby computed not only for the removal of a nucleon, but for energies above the Fermi level they refer to the addition of a nucleon. The gross features of the spectroscopic strengths as a function of energy are the same as in earlier calculations [5,7]. For orbits around the Fermi level, there is one solution with a large spectroscopic factor, called the quasiparticle state. The other solutions with small spectroscopic factors scatter over a wide energy range of several tens of MeV. The main difference between the present and earlier calculations is that the sum of the spectroscopic factors for removal of a particle from a certain orbit plus that for addition of a particle in that same orbit add up to only about 93% of the independent-particle shell model value. This is illustrated in Table II. The missing amount, about 7%, which is a consequence of the energy dependence of the Hartree-Fock (HF) energies (8), must be ascribed to orbits outside the model space. Table II illustrates that this energy dependence of the

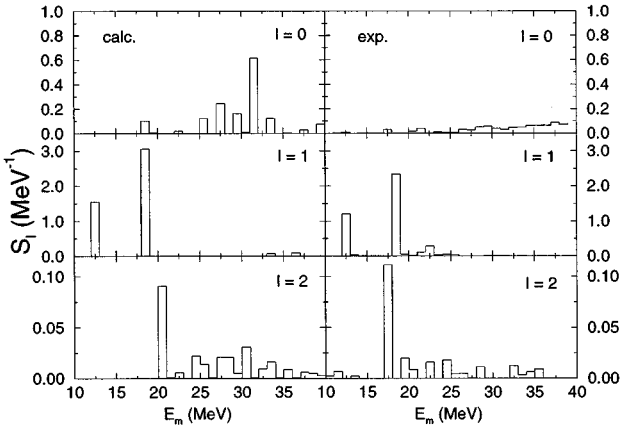

FIG. 3. The calculated one-proton removal strength as a function of the ''missing energy'' $E_m = E^{A-1} - E^A$ for ^{16}O for different l values (weighted with a factor $2j_\alpha + 1$) is compared with the measured one-hole spectral function of ^{16}O taken from [31].

HF energies reduces all parts of the strength by roughly the same factor.

A more detailed comparison with the spectroscopic strength deduced from $(e,e'p)$ data [31] is made in Fig. 3. This figure clearly shows that the calculated spectroscopic factors for the lowest $\frac{1}{2}^-$ and $\frac{3}{2}^-$ states ($l=1$) are still too large by about $15-20\,\%$ of the independent-particle shell model values. This discrepancy would have been 7% larger when the energy dependence of the G matrix, simulating the effect of short-range correlations, had been neglected.

One may think of several (partial) explanations for the remaining discrepancy. It could be that short-range correlations are not sufficiently dealt with by the present approach. However, their effect in the present work agrees with more direct calculations [12,26]. In [11] it was claimed that the quasihole peak is reduced by another 10% when the center-of-mass motion is treated properly. This result seems to be in contradiction with [32], in which it is argued that the spurriosity of the $1s$ state in ^{16}O actually leads to an enhancement of the spectroscopic factors for the $1p$ shells. Further work on this subject should clarify this issue.

A more likely shortcoming is that the treatment of long-range correlations is still not quite adequate. Figure 3 shows that the fragmentation of the $l=0$ strength as well as the side peaks for $l=1$ are underestimated by the calculations. It is not easy, however, to find a better, numerically still tractable, approximation for the self-energy [15]. The search for such an approximation should focus on complex structure at low energies, because the discrepancy between calculations and data is less for the integrated strength over the whole energy range up to 40 MeV. The data [31] gave 4.30 for $l=1$ and 0.254 for $l=2$ as compared to 4.78 and 0.261 for the calculations. The calculated spectral function for $l=2$ in Fig. 3 agrees rather nicely with the data, as its nonzero value is entirely due to correlations. Also for these orbits a larger role of collectivity at low energy would give a slight further improvement, viz. in this case a stronger concentration in the lowest (collective) state would be achieved.

IV. SUMMARY AND CONCLUSIONS

A method is proposed and applied to the nucleus ^{16}O to include the effect of both short- and long-range correlations in the calculation of the one-proton removal amplitudes by taking into account the energy dependence of the G matrix. Due to this energy dependence an extra depletion of the one-proton removal strength by somewhat less than 10% is found. The size of this effect is in agreement with a calculation of high-momentum components in ^{16}O [26]. The fragmentation by long-range correlations is described by the coupling to the 2h1p and 2p1h propagator in the Tamm-Dancoff approximation. The obtained fragmentation is too small for the $l=1$ strength which signals that not yet all the relevant low-energy dynamics is adequately incorporated. This was to be expected in view of the complicated excitation spectrum of the initial nucleus (^{16}O). The total $l=2$ hole strength in the experimentally explored energy range compares well with the data. The fragmentation of the deep-lying $l=0$ hole state probably requires a continuum description of the final nucleus, as its energy spectrum peaks well above the two-nucleon emission threshold.

The calculations might be improved using a larger model space for the long-range correlations. Also a Faddeev calculation in full space would be interesting. Extensions of the Faddeev approximation, to incorporate RPA-like (backward going) diagrams would be interesting too, but it is as yet unclear how that may be accomplished [15]. A point to be investigated further is the effect of the center-of-mass motion, which might be as large as 10%, but for which seemingly contradictory statements have been made [11,32].

ACKNOWLEDGMENT

Part of this work was supported by the U.S. National Science Foundation under Grant No. 9307484.

[1] J. W. A. den Herder *et al.*, Nucl. Phys. **A490**, 507 (1988).
[2] E. N. M. Quint, Ph.D. thesis, NIKHEF, Amsterdam, 1988.
[3] G. J. Kramer, Ph.D. thesis, NIKHEF, Amsterdam, 1990.
[4] G. van der Steenhoven, Nucl. Phys. **A527**, 17c (1991).
[5] M. G. E. Brand *et al.*, Nucl. Phys. A **531**, 253 (1991).
[6] G. A. Rijsdijk *et al.*, Phys. Rev. C **48**, 1752 (1993).
[7] D. van Neck, M. Waroquier, and J. Ryckebusch, Nucl. Phys. **A530**, 347 (1991).
[8] H. Müther and L. D. Skouras, Nucl. Phys. **A555**, 541 (1993).
[9] A. Ramos, A. Polls, and W. Dickhoff, Nucl. Phys. **A503**, 1 (1989).
[10] D. van Neck, A. E. L. Dieperink, and E. Moya de Guerra, Phys. Rev. C **51**, 1800 (1995).
[11] M. Radici, S. Boffi, S. C. Pieper, and V. R. Pandharipande, Phys. Rev. C **50**, 3010 (1994).
[12] H. Müther and W. H. Dickhoff, Phys. Rev. C **49**, R17 (1994).

[13] A. A. Abrikosov, L. P. Gorkov, and I. E. Dzyaloshinski, *Methods of Quantum Field Theory in Statistical Physics* (Dover, New York, 1963).
[14] A. L. Fetter and J. D. Walecka, *Quantum Theory of Many Particle Physics* (McGraw-Hill, New York, 1971).
[15] G. A. Rijsdijk, W. J. W. Geurts, K. Allaart, and W. H. Dickhoff, Phys. Rev. C **53**, 201 (1996).
[16] H. Müther and P. Sauer, in *Computational Nuclear Physics*, edited by K.-H. Langanke, J. A. Maruhn, and S. E. Koonin (Springer, Berlin, 1993).
[17] R. Machleidt, Adv. Nucl. Phys. **19**, 191 (1989).
[18] M. Lacombe, B. Loiseaux, J. M. Richard, R. Vinh Mau, J. Côté, P. Pirès, and R. de Tourreil, Phys. Rev. C **21**, 861 (1980).
[19] R. B. Wiringa, R. A. Smith, and T. L. Ainsworth, Phys. Rev. C **29**, 1207 (1984).
[20] R. Reid, Ann. Phys. **50**, 411 (1968).
[21] H. Müther, G. Knehr, and A. Polls, Phys. Rev. C **52**, 2955 (1995).
[22] M. Baldo, I. Bombaci, G. Giansiracusa, U. Lombardo, C. Mahaux, and R. Sartor, Nucl. Phys. **A545**, 741 (1992).
[23] I. E. Lagaris and V. R. Pandharipande, Nucl. Phys. **A359**, 331 (1981).
[24] O. Benhar, A. Fabrocini, and S. Fantoni, Phys. Rev. C **41**, R24 (1991).
[25] B. E. Vonderfecht, W. H. Dickhoff, A. Polls, and A. Ramos, Nucl. Phys. **A555**, 1 (1993).
[26] H. Müther, A. Polls, and W. H. Dickhoff, Phys. Rev. C **51**, 3040 (1995).
[27] G. A. Rijsdijk, K. Allaart, and W. H. Dickhoff, Nucl. Phys. **A550**, 159 (1992).
[28] J. Winter, Nucl. Phys. **A194**, 535 (1972).
[29] P. Schuck, F. Villars, and P. Ring, Nucl. Phys. **A208**, 302 (1973); Phys. Rev. C **29**, 1207 (1984).
[30] J. Yuan, Ph.D. thesis, Washington University, St. Louis, 1994.
[31] M. Leuschner *et al.*, Phys. Rev. C **49**, 955 (1994).
[32] A. E. L. Dieperink and T. de Forest, Jr., Phys. Rev. C **10**, 543 (1974).